Metal, **65**, 261 (1974a).
Predel, Bruno, and Günther Oehme, "Thermodynamic Properties of Liquid Hg-Tl Alloys with Regard to an Equilibrium of Association," *Z. Metal*, **65**, 509 (1974b).
Predel, Bruno, and Günther Oehme, "Investigation of the Effect of Association on the Concentration Dependence of the Enthalpy of Mixing of Liquid Hg-In Alloys," *Z. Metal*, **65**, 525 (1974c).
Prigogine, I., and R. Defay, "Chemical Thermodynamics," translated by D. H. Everett, Longmans, Green and Co., New York, 409 (1954).
Rao, Y. K., and G. R. Belton, "Thermodynamic Properties of Mg-Ge Alloys," *Met. Trans.*, **2**, 2215 (1971).
Sharma, R. A., "Thermodynamic Properties of Liquid Mg + Pb and Mg + Sn Alloys by e.m.f. measurements," *J. Chem. Thermodyn.*, **2**, 373 (1970).
Smith, J. S., "Chemical Theory and EMF Studies of Highly Solvated Liquid Metal Systems," Ph.D. Thesis, University of Illinois, Urbana (1975).
F. Sommer, "Influence of Associate Formation in Alloy Melts on the Thermodynamic Quantities," *Calphad*, **2**, 319 (1978).
Steiner, A., E. Miller, and K. L. Komarek, "Magnesium-Tin Phase Diagram and Thermodynamic Properties of Liquid Magnesium-Tin Alloys," *Trans. Met. Soc. AIME*, **230**, 1361 (1964).
Stroup, P. T., "Carbothermic Smelting of Aluminum," *Trans. Met. Soc. AIME*, **230**, 356 (1964).
Trotter, P. J., and D. A. Yphantis, "Multiple Equilibria in Donor-Acceptor Complexing Studied by Ultracentrifugation," *J. Phys. Chem.*, **74**, 1399 (1970).
Wilhelm, H. A., "The Carbon Reduction of Uranium Oxide," USAEC R & D Report IS-1023, Metals, Ceramics, and Materials, UC-25 (1964).

Manuscript received October 8, 1980; revision received May 18, and accepted June 22, 1981

Hydrogenation of Nitrobenzoic Acid

Aqueous solutions of *p*-nitrobenzoic acid were hydrogenated in the presence of Pt/C and Pd/C catalysts in a slurry reactor. External as well as internal mass transport steps were studied using a membrane H_2-electrode and a metal probe electrode. After the influence of the mass transport effects was corrected for, it was possible to obtain corrected values of the kinetic characteristics of the overall chemical reaction. The mechanism was studied using potential and polarization methods.

BENGT ANDERSSON

Department of Chemical Reaction Engineering
Chalmers University of Technology
Göteborg, Sweden

SCOPE

Kinetic studies in liquid phase hydrogenations to obtain true kinetic characteristics of the chemical steps as activation energy and reaction orders are difficult to perform due to the influence of mass transport limitations in the phase interfaces and in the pore system of the catalyst. Since it is very difficult to eliminate these transport hindrances, the best way to study the kinetics of this system should be to determine directly the substrate concentration or to estimate the concentration decreases due to the transport effects. Owing to its low concentration in liquid phase, hydrogen is more affected by transport limitations than other reactants, so a direct measurement of the hydrogen concentration is of primary importance.

Recently a H_2-membrane electrode was constructed and tested (Andersson and Berglin, 1981a) for hydrogen concentration determinations under liquid phase hydrogenation conditions. A corresponding metal probe electrode was also tested (Andersson, 1981) for the determination of local catalyst potentials and, subsequently, also for the hydrogen activity of the catalyst. By using these two electrodes it was possible to study the chemical kinetics and the mechanism of nitrobenzoic acid hydrogenation in aqueous medium in more detail.

CONCLUSIONS AND SIGNIFICANCE

Much effort has been made to minimize errors in the kinetic parameters due to the influence from mass transfer. The difficulty in estimating the gas-liquid mass transfer resistance was eliminated by measuring the hydrogen concentration in the liquid phase with the hydrogen membrane electrode. The liquid to particle and the intraparticle mass transport resistances were minimized by using very small catalyst particles with a mean diameter less than 1.5 μm. The intraparticle resistance could not be eliminated completely, but since the effective diffusivity was measured and the particle size distribution could be obtained, this resistance was estimated and compensated for in the kinetic evaluation. The liquid to particle mass transfer was estimated from an assumed Sherwood number. This resistance was very small and consequently, the value of the assumed Sherwood number was not critical.

The hydrogenation of nitrobenzoic acid showed a first order dependence with respect to hydrogen concentration and zero order with respect to the concentration of nitrobenzoic acid. The activation energy was found to be 36 kJ/mol both for 1% Pd/C and 5% Pd/C with the same dispersion, even though the reaction on 5% Pd/C was strongly influenced by an intraparticle mass transfer resistance. This result showed that the intraparticle mass transport is correctly estimated.

Wagner (1970) outlined some electrochemical methods which were used in this mechanistic study of the hydrogenation of nitrobenzoic acid. By studying the catalyst potential it was found that most of the available Gibbs' energy was used in adsorption and dissociation of hydrogen and it seems reasonable to assume that the dissociation of hydrogen is the rate determining step. Polarographic measurements on Pt reveal that nitrobenzoic acid and its reaction intermediates cover 80–90% of the active surface of the catalyst.

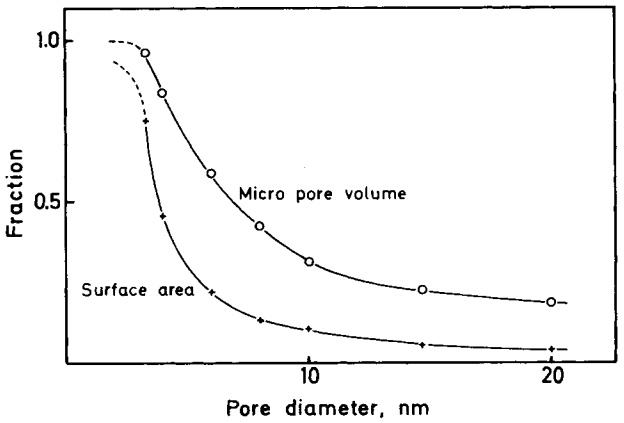

Fig. 1 Pore size distribution.

THEORY

Rate Determining Steps in Liquid Phase Hydrogenation

The rate determining steps in liquid phase hydrogenation of nitrobenzoic acid in a slurry reactor are mass transport steps and chemical steps. In the present investigation, the product of the substrate concentration and its diffusivity was much higher than that of dissolved hydrogen, so substrate and product mass transfer were considered insignificant. The main mass transport steps will then be the transport of hydrogen from the gas phase through the liquid to the active metal on the support. The first slow step in this sequence is transport of hydrogen through the liquid film surrounding the gas bubble. The rate of this transport can be written

$$\mathrm{Na} = k_L a \left(\frac{P_{\mathrm{H_2}}}{\mathrm{He}} - c_b\right) \text{ mol/s m}^3 \tag{1}$$

The transport through the film surrounding the catalyst particle may be written

$$NSm = k_s S(cnb - c_s)m, \text{ mol/s m}^3 \tag{2}$$

The rate of hydrogen transport through the pores of the catalyst particle coupled with the simultaneously occuring chemical reaction follows the equation

$$r = \eta \cdot k_v \cdot c_s^{\alpha} \cdot c\frac{\beta}{\mathrm{RNO_2}} \cdot m \text{ mol hydrogen/s m}^3 \tag{3}$$

with

$$k_v = A \cdot \exp(-E_a/RT)$$

In Eq. 3 the effectiveness factor η summarizes the influence of the pore effect on chemical kinetics. The effectiveness factor can be expressed as a function of the Thiele modulus.

For spherical geometry the Thiele modulus is defined as

$$\phi = \frac{d_p}{2}\left[\frac{\alpha+1}{2} \cdot \frac{k_v c_s^{\alpha-1}\, {}^{\beta}_{\mathrm{RNO_2}}}{D_{\mathrm{eff}}}\right]^{1/2} \tag{4}$$

For $\alpha = 1$, $\cdot c^{\beta}_{\mathrm{RNO_2}}$ constant, and spherical geometry, the effectiveness factor can be calculated from

$$\eta = \frac{3}{\phi}\left(\frac{1}{\tanh\phi} - \frac{1}{\phi}\right) \tag{5}$$

The observed reaction orders and activation energy will be affected by the presence of a pore transport resistance.

However, if we compensate for mass transport by determining the effectiveness factor, it is possible to obtain the true reaction orders and also the true activation energy.

In this investigation, a size dispersed catalyst has been used. When the reaction rate is first order we can calculate a Thiele modulus valid for this dispersion. For small values of ϕ Pratt and Wakeham (1975) have deduced

$$\phi = \phi_{gm} \exp(4\sigma_g^2) \frac{\mathrm{erf}\left(\frac{N_2}{\sqrt{2}} - \frac{5\sigma_g}{\sqrt{2}}\right) + \mathrm{erf}\left(\frac{N_1}{\sqrt{2}} + \frac{5\sigma_g}{\sqrt{2}}\right)}{\mathrm{erf}\left(\frac{N_2}{\sqrt{2}} - \frac{3\sigma_g}{\sqrt{2}}\right) + \mathrm{erf}\left(\frac{N_1}{\sqrt{2}} + \frac{3\sigma_g}{\sqrt{2}}\right)} \tag{6}$$

and for large values of ϕ

$$\phi = \phi_{gm} \exp[(5/2)\sigma_g^2] \frac{\mathrm{erf}\left(\frac{N_2}{\sqrt{2}} - \frac{3\sigma_g}{\sqrt{2}}\right) + \mathrm{erf}\left(\frac{N_1}{\sqrt{2}} + \frac{3\sigma_g}{\sqrt{2}}\right)}{\mathrm{erf}\left(\frac{N_2}{\sqrt{2}} - \sqrt{2}\cdot\sigma_g\right) + \mathrm{erf}\left(\frac{N_1}{\sqrt{2}} + \sqrt{2}\cdot\sigma_g\right)} \tag{7}$$

where ϕ_{gm} is the Thiele modulus for the geometric mean (number basis) and σ_g the standard deviation in a log-probability plot of the distribution. N_1 and N_2 are the number of logarithmic standard deviations from the mean corresponding to the lower and upper particle size limits, respectively.

When the entire distribution of sizes is present ($N_1 = N_2 = \infty$) Eqs. 6 and 7 are reduced to

$$\phi = \phi_{gm} \exp[4\sigma_g^2] \tag{8}$$

and

$$\phi = \phi_{gm} \exp[(5/2)\sigma_g^2] \tag{9}$$

EXPERIMENTAL

Four different catalysts were used: 1% Pt/C, 1% Pd/C, 3% Pd/C, and 5% Pd/C. The support has the same characteristics for all four catalysts. For kinetic and catalyst potential measurements a crushed sieve fraction <20 μm was used.

The pore size distribution of the charcoal support was measured by nitrogen sorption using a glass vacuum system. The distribution was computed using the method of Anderson (1968). The metal area of catalyst was determined using the hydrogen titration method according to Wilson and Hall (1970). The particle size distribution was measured with a Coulter counter (Allen, 1974).

The hydrogenation of nitrobenzoic acid was performed in 0.2 M phosphate buffer at pH 6 in a glass reactor similar to that described by Furusawa and Smith (1973). High pressure tests were performed in a stainless steel autoclave. The hydrogen pressure was varied between 0.1 bar and 5 bar.

The reactants were analysed by LC with a Perkin-Elmer Ion X SA, Anionic Ion Exchanger. The mobile phase was 0.2 M phosphate buffer at pH 6. Only nitro- and aminobenzoic acids were observed.

The hydrogen concentration in the solution was measured with a membrane electrode (Andersson and Berglin, 1981).

The potential of the catalyst was measured by introducing a silver rod into the solution. The catalyst particles then collide with the rod and transfer their potentials, which were measured with a calomel electrode as a reference.

Polarization measurements in the mechanistic study were performed with a PAR 174 polarograph. The working electrode was a fixed 1 cm^2 Pt-foil. The counterelectrode was a 10 cm^2 Pt-foil and a calomel electrode was used as a reference. All measurements were performed in 0.2 M phosphate buffer pH 6. Heavy agitation (3,000 rpm) was maintained in order to minimize the mass transfer resistance. No polarization measurements were performed on palladium due to the high solubility of hydrogen in this metal, which makes it difficult to evaluate the results.

RESULTS

Catalyst Characterization

Cumulative pore volume and surface area as a function of pore size are shown in Figure 1. BET area and pore volume data are presented in Table 1.

The size distribution of the catalyst used for the kinetic experiments fitted very well to a straight line in a log-normal distribution plot, as can be seen for 1% Pt/C in Fig. 2. The other catalysts have

TABLE 1. PROPERTIES OF THE CATALYST SUPPORT

Surface Area m^2/kg	Porosity	Mean Pore Diameter nm
$8 \cdot 10^5$	0.62	3.5

similar distributions. These results and the results from the metal surface area measurements are given in Table 2.

Kinetic and Mass Transport Measurements

The mass transport resistance must be taken care of in order to obtain the true parameters in the rate equation.

Since the hydrogen concentration in the bulk solution was measured directly by the membrane electrode, the analysis of the experiments was not influenced by the mass transport step in the gas-liquid interphase. At 50°C $k_L a$ was measured independently (Andersson, 1981) and found to be 0.44 s^{-1} at 1,400 rpm in the actual laboratory reactor. This result agrees well with the results obtained from concentration measurement during the kinetic experiments.

For liquid-solid mass transfer the Sherwood number was assumed to be Sh = 3. This value is lower than other reported values for carbon suspensions. Other authors [8] most often give the value Sh = 4. It should be noted, however, that much smaller particles are used in the present investigation, which may explain the lower value chosen here. Bulk diffusivity was determined using the Taylor dispersion method (Andersson and Berglin, 1981b). The diffusivity of hydrogen in this solution was found to be

$$D_{H_2} = 4.4 \cdot 10^{-9} \exp\left[1392 \left\{\frac{1}{298} - \frac{1}{T}\right\}\right] m^2/s$$

The intraparticle mass transfer resistance could be calculated from Eq. 5 since the reaction order with respect to hydrogen concentration was found to be close to unity. Effective diffusivity of hydrogen in water filled carbon catalyst was determined at 50°C to be $7.4 \cdot 10^{-10}$ m^2/s (Andersson, 1977). We assume the same

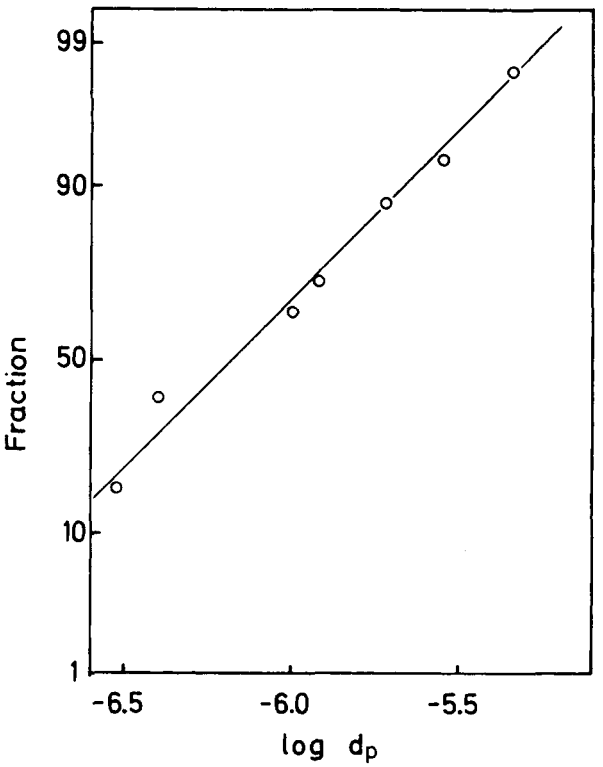

Fig. 2 Log-normal particle size distribution.

TABLE 2. PROPERTIES OF THE CATALYST

Catalyst	d_{gm} μm	σ_g	Metal Dispersion
1% Pt/C	0.71	0.38	0.31
1% Pd/C	1.22	0.42	0.23
3% Pd/C	1.02	0.44	0.38
5% Pd/C	1.42	0.48	0.22

temperature dependance for effektive diffusivity as for bulk diffusivity. With Eqs. 2, 3, 4, 5 and 8 the parameters in Eq. 3 was obtained from experimental data using non-linear least squares regression. The result is presented in Table 3. The limits given are approximative 95% confidence intervals.

The activation energy E_a is corrected for the changes in the solubility of hydrogen and in the partial pressure of water with temperature. Since we compensate for mass transfer in the regression, the true reaction orders and activation energy were obtained.

The results were divided into two parts, one for the fraction of catalyst with small crushed particles and one for larger size particles. The first fraction of particles is here called the kinetic fraction, since it was used in the kinetic experiments. All experiments were performed with a catalyst load of 50 mg/L for 5% Pd/C and 100 mg/L for the other catalysts.

The mass transfer resistance in the gas-liquid interphase was calculated directly from the membrane electrode measurements of the hydrogen concentration in the bulk liquid (c_b). The concentration of saturated solution (p_{H_2}/He) was measured in a similar way in a solution without the catalyst. From Table 4, column 5, it is seen that the mass transfer resistance in the liquid-gas interface is small in most experiments.

The liquid-catalyst mass transfer was estimated from the assumption that the Sherwood number was Sh = 3 for the kinetic fraction of the catalyst and Sh = 4 for the large particles. As may be seen from Table 4, the mass transfer resistance near the catalyst external surface is very small for the kinetic fraction of the catalyst. Liquid-solid mass transport has only an effect for larger particles. The assumption Sh = 3 is consequently not a critical one.

In order to calculate the effectiveness factor η, the distribution of the particle size of the slurry must be considered, since the Thiele modulus is a function of the particle size. From the mean particle size and its distribution it is possible to calculate a corrected Thiele modulus from Eqs. 6–9. The geometric mean Thiele modulus ϕ_{gm} and the corrected Thiele modulus ϕ are given in Table 4. Using the corrected Thiele modulus it is now possible to calculate the effectiveness factor η from Eq. 5. As seen from Table 4, η is close to unity for 1% Pd/C and 1% Pt/C of the kinetic fraction of the catalyst. It is obvious from this result that these catalysts may be used to further investigate the reaction mechanism. On the other hand, the effectiveness factor for the 5% Pd/C catalyst was rather low ($\eta = 0.77$), which is explained by the fact that the amount of active metal is very high. It is interesting to note that the activation energy (Table 3) was the same for 5% Pd/C and 1% Pd/C, which shows that the kinetic data was corrected for the mass transfer influence in a proper way. It also indicates that the same rate determining step is operating for both catalysts. Also 3% Pd/C gives the same reaction rule/active surface which indicates that the reaction is structure insensitive.

The calculation of η was checked using the assumption that there were no pore transport limitations in the experiments with the first catalyst in Table 4. The measured effectiveness catalyst $\eta_{meas.}$ can be evaluated by comparing the reaction at the same concentration of hydrogen at the surface of the catalyst. It is seen from Table 4 that η agrees very well with $\eta_{meas.}$, which indicates that η may be correctly calculated from Eq. 5 and that D_{eff} is properly determined.

Mechanism of the Chemical Reaction

Wagner (1970) outlined some methods to study the mechanism of hydrogenation in the presence of the noble metal catalysts. Some

TABLE 3. RESULTS OF THE KINETIC MEASUREMENTS

Catalyst	$k_v \cdot 10^{-2}$ (50°C)	$A \cdot 10^{-8}$ s^{-1}	E_a kJ	α	β
1% Pt/C	1.0	—	—	1.11 ± 0.11	0.02 ± 0.02
1% Pd/C	2.5	1.65 ± 0.84	35.9 ± 4.2	1.04 ± 0.06	0.01 ± 0.01
3% Pd/C	12	—	—	0.98 ± 0.11	0.04 ± 0.06
5% Pd/C	11	8.72 ± 5.1	36.4 ± 5.1	0.94 ± 0.11	0.04 ± 0.02

of his suggestions are applied to the hydrogenation of nitrobenzoic acid below.

Consider the reaction sequence

$$H_2(g) \rightarrow H_2(aq) \quad (1')$$

$$H_2(aq) \rightarrow H_2(ad) \quad (2')$$

$$H_2(ad) \rightarrow 2H(ad) \quad (3')$$

$$H(ad) \rightarrow H^+(ad) + e^- \quad (4')$$

$$RNO_2(aq) \rightarrow RNO_2(ad) \quad (5')$$

and

$$RNO_2(ad) + 6H^+ + 6e^- \rightarrow RNH_2(ad) + 2H_2O \quad (6a')$$

$$RNO_2(ad) + 6H(ad) \rightarrow RNH_2(ad) + 2H_2O \quad (6b')$$

$$RNH_2(ad) \rightarrow RNH_2(aq) \quad (7')$$

In order to differentiate between mechanisms 6a′ and 6b′ one may firstly investigate the rate of the overall reaction:

$$RNO_2 + 3H_2 \rightarrow RNH_2 + 2H_2O \quad (8')$$

as a function of the concentration of reactants. Secondly, one may measure the steady state catalyst potential and the steady state hydrogen atom activity as a function of the concentration of reactants. Thirdly, one may investigate the polarization characteristics of the noble metal electrode.

Potential Measurements

The equilibrium potentials E'_{eq} and E''_{eq} correspond to the reactions

$$H_2(g) \rightleftarrows 2H^+(aq) + 2e^-$$

and

$$2H_2O + RNH_2(aq) \rightleftarrows RNO_2(aq) + 6H^+(aq) + 6e^-$$

The corresponding potentials are given by Nernst's law

$$E'_{eq} = \frac{RT}{2F} ln \frac{\{H^+\}^2}{P_{H_2}} \quad (10)$$

and

$$E''_{eq} = E''^0_{eq} + \frac{RT}{6F} ln \frac{\{RNO_2\}\{H^+\}^6}{\{RNH_2\}}, \quad (11)$$

respectively.

The steady-state potential E_{st} is the potential obtained on the catalyst when reaction 8′ proceeds. This reaction is not in equilibrium and Nernst's law cannot be applied. However, step (Eq. 4′) in this reaction sequence is fast and considered in equilibrium. Nernst's law can thus be applied to that step giving:

$$E_{st} = E^0 + \frac{RT}{F} ln \frac{\{H^+\}^2}{\{H_{st}(ad)\}} \quad (12)$$

The activity of adsorbed hydrogen can be calculated from

$$\frac{\{H_{st}(ad)\}}{\{H_{eq}(ad)\}} = \exp\left[\frac{-(E_{st} - E'_{eq}) \cdot F}{RT}\right] \quad (13)$$

Figure 3 shows $E_{st} - E'_{eq}$ and $E''_{eq} - E'_{eq}$ during a normal hydrogenation. The change in Gibbs' energy of the overall reaction may be written

$$\Delta G = -6F(E''_{eq} - E'_{eq}) \quad (14)$$

Since ΔG must be negative, we have $E''_{eq} > E'_{eq}$. The change in Gibbs' energy for the first four steps (Eqs. 1′-4′) is given by

$$\Delta G_{1-4} = -6F(E_{st} - E'_{eq}) \quad (15)$$

and for the remaining steps

$$\Delta G_{5-7} = -6F(E''_{eq} - E_{st}) \quad (16)$$

The steady-state potential E_{st} can consequently indicate in which part of the reaction sequence the rate determining step (rds) is to be found. Since all equations including RNO_2 and RNH_2 will be simplified if $\{RNO_2\} = \{RNH_2\}$, the following discussion concerns 50% conversion. In Figure 3, 50% conversion is obtained after about 1,000 s of reaction. At 50% conversion we obtain from Eqs. 14 and 15 and Figure 3:

$$\Delta G_{1-4} = 179.5 \text{ kJ/mol } RNO_2$$

and

$$\Delta G_{5-7} = 98.4 \text{ kJ/mol } RNO_2$$

Since ΔG_{1-4} and ΔG_{5-7} are large, we may conclude that both the reaction sequence 1–4 and the reaction sequence 5–7 are far from being in equilibrium.

The mass transport step of hydrogen is step (1′). A change in mass transport of hydrogen will consequently affect E_{st}. For 1% Pd/C and 1% Pt/C practically no change in catalyst potential was obtained when the impeller speed varied between 1,000 rpm and 2,000 rpm. For 5% Pd/C a somewhat larger effect was noticed. This is probably due to a change in $k_L a$ with impeller speed and is in good agreement with the result in Table 4.

A linear relationship was obtained between the steady state catalyst potential and the logarithm of hydrogen pressure at 50% conversion (Figure 4). Since we have a first order dependence of hydrogen concentration of reaction rate, there is also a linear de-

TABLE 4. MASS TRANSPORT RESISTANCES AT 50°C

Catalyst	Sieve Fraction μm	d_{gm} μm	Reaction Rate (r) mol H_2/ s kg cat.	$\frac{c_b \text{ He}}{P_{H_2}}$	$\frac{c_s}{c_b}$	ϕ_{gm}	ϕ	η	$\eta_{meas.}$
1% Pd/C	kinetic	1.22	0.217	0.91	0.96	0.31	0.71	0.97	1
1% Pd/C	32–40	34	0.0408	0.98	0.69	9.93	10.51	0.26	0.27
1% Pd/C	40–50	42	0.0309	0.98	0.65	12.27	12.85	0.22	0.22
1% Pd/C	50–72	55	0.0177	1.00	0.65	16.07	18.12	0.16	0.13
5% Pd/C	kinetic	1.42	0.729	0.87	0.95	0.89	2.27	0.77	—
1% Pt/C	kinetic	0.78	0.0906	0.96	0.99	0.14	0.26	0.99	—

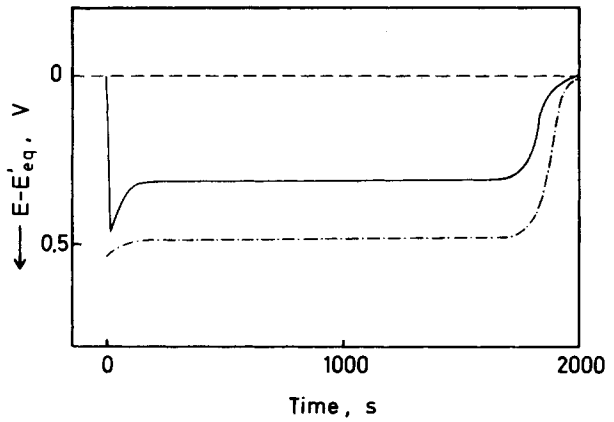

Fig. 3 Catalyst potential as a function of time during a normal hydrogenation (—) E_{st} and (- • - •) E''_{eq}

pendence between E_{st} and the logarithm of reaction rate. This relationship may be written

$$r = k \exp\left[-\frac{\alpha F}{RT}(E_{st} - E''_{eq})\right] \tag{17}$$

Equation 17 can be used to study the mechanism of the steps (5′)-(7′). The charge transfer coefficient α shows how sensitive the reaction rate is to a variation in the catalyst potential. A high value of the coefficient is obtained when electrochemical charge transfer steps are slow, while a low value is obtained when nonelectrochemical steps are slow. From Figure 4 the charge transfer coefficient from 1% Pt/C was found to be $\alpha = 0.35$. This is neither a high nor a low value from a mechanistic point of view, so the rate determining step for the sequence (5′)-(7′) is probably a combination of electrochemical (charge transfer) and non electrochemical steps.

Polarization Measurements

Further information concerning the reaction mechanism may be obtained from polarization measurements. Polarization curves for hydrogen, nitrobenzoic acid and for nitrobenzoic acid in the presence of hydrogen were determined (Figure 5).

Moreover, the polarization measurements were performed in solutions with equal concentrations of nitrobenzoic acid and aminobenzoic acid, i.e., at 50% conversion. The polarization curve for hydrogen is assumed to fit Eq. 12.

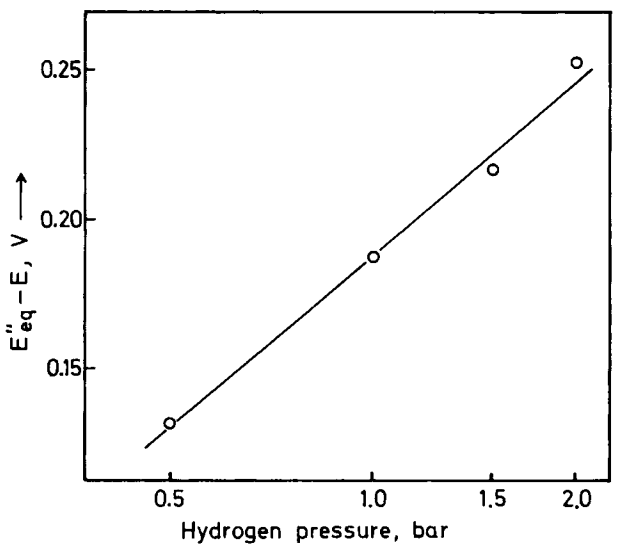

Fig. 4 The steady-state catalyst potential as a function of hydrogen pressure

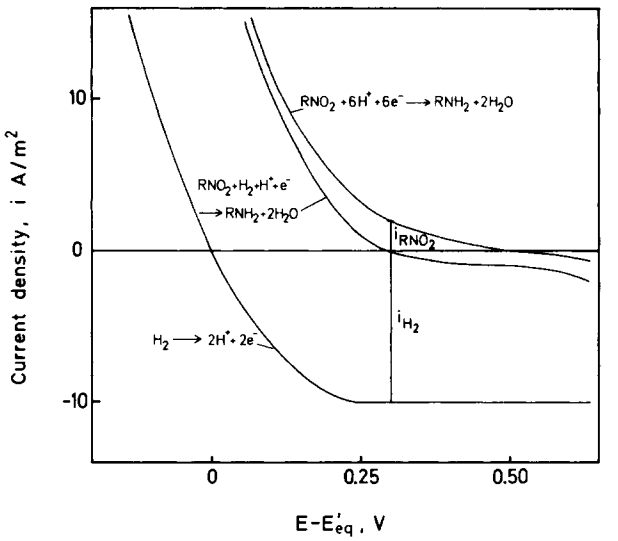

Fig. 5 Polarization curves for hydrogen at 1 bar, 0.1 M nitrobenzoic acid, and 0.1 M aminobenzoic acid in the presence of hydrogen at 1 bar.

$$i = k_1 c_{H_2}(1 - \theta_H)^2 - k_{-1}\theta_H^2 \tag{18}$$

The polarization curve levels out for $E - E'_{eq} \approx 0.25$V, i.e., when the fraction of hydrogen (θ_H) approaches zero. The rate determining step is obviously the dissociation of hydrogen.

The current in the electrochemical reduction of nitrobenzoic acid, Figure 5, fits the equation

$$i = k_2 \exp\left[-\frac{\alpha F}{RT}(E - E''_{eq})\right] \tag{19}$$

with $\alpha = 0.33$, which is very close to the charge transfer coefficient $\alpha = 0.35$ obtained from hydrogen pressure variations, as found above. The rate constant k_2 is almost constant for $c_{RNO_2} > 10$ mM, but is gradually smaller for lower concentrations.

At E_{st} the rate of production of electrons must be equal to the rate of consumption of electrons. Assuming that the function of the catalysts not covered by nitrobenzoic acid or reaction intermediates of nitrobenzoic acid, is available for hydrogen dissociation we can write

$$(1 - \theta_{RNO_2})\, i_{H_2} = \theta_{RNO_2} \cdot i_{RNO_2} \tag{20}$$

From this equation we can calculate θ_{RNO_2}.

Wagner (1970) concluded that if $i_{RNO_2} \approx 6$ F times the rate of hydrogenation/active surface area, an electrochemical mechanism prevails. This is unfortunately not valid for platinum, since the reverse of reaction (4′) is rapid. Hydrogen atoms may be formed in that reaction and react further with nitrobenzoic acid. Still, it is of interest to note that 6 Fr = 2.0 A/m². Polarographic reduction and hydrogenation gives the same reaction rate at the same potential.

NOTATION

a = gas-liquid specific interface area, m²/m³
c_b = bulk concentration of hydrogen, mol/m³

TABLE 5. RESULTS OF POLARIZATION EXPERIMENTS AT STEADY STATE

P_{H_2} bar	c_{RNO_2} mM	$E_{st} - E'_{eq}$ V	i_{H_2} A/m²	i_{RNO_2} A/m²	θ_{RNO_2}
1.0	1	0.297	10	8.9	0.53
1.0	10	0.311	10	1.4	0.88
1.0	50	0.309	10	2.2	0.82
1.0	100	0.307	10	1.6	0.86

All experiments are performed at $c_{RNO_2} = c_{RNH_2}$.

c_s = concentration of hydrogen in the liquid-solid interface, mol/m^3
D_{eff} = effective diffusivity, m^2/s
d_{gm} = geometric mean particle diameter (number basis), m
E_a = activation energy, kJ/mol
E_D = activation energy of diffusion, kJ/mol
E = electrochemical potential, V
F = Faraday's constant, As/mol
He = Henry's constant, bar·m^3/mol
i = current density, A/m^2
k_v = rate constant, (s·m^3 catalyst)$^{-1}$
m = catalyst loading, m^3/m^3
N = rate of mass transfer, mol/s·m^2
N_1, N_2 = number of logarithmic standard deviations from the mean corresponding to a lower and an upper particle size limit, respectively
RNH_2 = aminobenzoic acid
RNO_2 = nitrobenzoic acid
S = liquid-catalyst specific external surface area, m^2/m^3
α = charge transfer coefficient
η = effectiveness factor
θ_H = fractional coverage of hydrogen
θ_{RNO_2} = fractional coverage of nitrobenzoic acid and reaction intermediates of nitrobenzoic acid
σ_g = standard deviation of the log-normal particle size distribution
ϕ = Thiele modulus (Eqs. 10–13)
ϕ_{gm} = Thiele modulus corresponding to particle of size d_{gm}

LITERATURE CITED

Acres, G. J. K. and B. J. Cooper, "Carbon-Supported Platinum Metal Catalysts for Hydrogen Rections," *J. Appl. Chem. Biotechnol.*, **22**, 769 (1972).

Allen, T., "Particle Size Measurements," p. 301, Chapman & Hall, London, England (1974).

Anderson, R. B., "Experimental Methods in Catalytic Research," p. 45, Academic Press Inc., New York (1968).

Andersson, B., "Mass Transfer and Reaction in a Slurry Reactor," Thesis, Chalmers University of Technology, Göteborg, Sweden (1977).

Andersson, B., "Fluid to Particle Mass Transfer in Slurries," Accepted to be published in *Chem. Eng. Sci.* (1981).

Andersson, B. and T. Berglin, "On the Theory and Use of a new Fast-Response Dissolved Hydrogen Probe for Hydrogen Transfer Studies," Accepted to be published in *Chem. Eng. J.* (1981a).

Andersson, B. and T. Berglin, "Dispersion in Laminar Flow through a Circular Tube," Accepted to be published in *Proceedings* of the Royal Society of London (1981b).

Bockris, J. O. M. and A. K. N. Reddy, "Modern Electrochemistry," p. 1231, Plenum Press, New York (1970).

Furusawa, T. and J. M. Smith, "Fluid-Particle and Intraparticle Mass Transport Rates in Slurries," *Ind. Eng. Chem. Fund.*, **12**, 197 (1973).

Pratt, K. C. and W. A. Wakeham, "Effektiveness Factors for a Size Dispersed Catalyst," *Chem. Eng. Sci.*, **30**, 444 (1975).

Wagner, C., "Considerations on the Mechanism of the Hydrogenation of Organic Compounds in Aqueous Solutions on Noble Metal Catalysts," *Electrochemia Acta*, **15**, 987 (1970).

Wilson, G. R. and W. K. Hall, "Studies of the Hydrogen Held by Solids," *J. Catal.*, **17**, 190 (1970).

Manuscript received December 4, 1979; revision received June 2, and accepted June 22, 1981

R&D NOTES

Laminar Free Convection with Suction or Blowing Along a Vertical Surface

TSAI-TSE KAO

FW Energy Applications, Inc.
Livingston, NJ 07039

In the past, the effects of suction or blowing on laminar free convection flow over a vertical porous plate have been the subject of several investigations. Eichhorn (1960) investigated the particular distributions of surface temperature and transpiration rates which lead to similarity solutions of the laminar boundary-layer equations. Corresponding to a wall temperature with power law distribution, it was found that similarity solutions were possible only when the blowing velocity $V_w \sim X^{(n-1)/4}$. Sparrow and Cess (1961) had presented an approximate series solution for the case of uniform transpiration and wall temperature. These authors also provided a transformation to be used when both wall temperature and transpiration velocities vary with different powers of X. More recently, numerical solutions for the case of constant wall temperature and transpiration rate had been obtained by Merkin (1972), Clarke (1973), and Parikh et al (1974). Kao (1976) had solved the same problem using Sparrows' two-equation local non-similar method. The more general problem of laminar free convection with arbitrarily prescribed transpiration rate will be investigated here using the strained co-ordinates technique of Kao, Domoto and Elrod (1977).

ANALYSIS

As a starting point, the set of conservation equations governing laminar free convection adjacent to a vertical wall will be transformed into the following:

$$f''' + (3 - 2\tilde{\beta})ff'' - 2f^{12} + \theta = 4\xi\left[f'\frac{\partial f'}{\partial \xi} - f''\frac{\partial f}{\partial \xi}\right] \quad (1)$$

$$\frac{1}{\mathrm{Pr}}\theta'' + (3 - 2\tilde{\beta})f\theta' - 4\tilde{\beta}f\theta = 4\xi\left[f'\frac{\partial \theta}{\partial \xi} - \theta'\frac{\partial f}{\partial \xi}\right] \quad (2)$$

$$(3 - 2\tilde{\beta})f(\xi,0) + 4\xi\frac{\partial f}{\partial \xi}(\xi,0) = \gamma(x) = -\frac{V_w X}{\nu}\left[\frac{4}{Gr_x}\right]^{1/4}$$

$$f'(\xi,0) = 0, \qquad \theta(\xi,0) = 1 \quad (3)$$

$$f'(\xi,\infty) = 0 \qquad \theta(\xi,\infty) = 0 \quad (4)$$